



# Graphite nanoparticles paper supercapacitor based on gel electrolyte

L. Fekri Aval<sup>1</sup> · M. Ghoranneviss<sup>1</sup> · G. Behzadi Pour<sup>2</sup>

Received: 9 July 2018 / Accepted: 8 October 2018 / Published online: 13 October 2018  
© The Author(s) 2018

## Abstract

In this study, three-type paper supercapacitors based on the polyvinylidene fluoride (PVDF) and polyvinyl alcohol (PVA)/phosphoric acid ( $H_3PO_4$ ) gel electrolytes and graphite nanoparticles (GNPs) electrodes have been fabricated. The gel electrolytes and electrodes films have been coated on the paper using push coating and then characterized by scanning electron microscopy (SEM). In two types of the paper supercapacitors, on the PVDF gel electrolyte film, a layer of PVA/water and  $BaTiO_3$  as a gel separator film has been coated. The specific capacitance of the paper supercapacitors using cyclic voltammetry (CV) and galvanostatic (charge–discharge) methods at the scan rates 20 and 150  $mV s^{-1}$  have been investigated. The paper supercapacitor based on the  $BaTiO_3$  separator film showed higher specific capacitance ( $312 F g^{-1}$ ) compared to other samples. Also, using electrochemical impedance spectroscopy (EIS), the Nyquist and Bode curves of paper supercapacitors have been measured. For the paper supercapacitors based on the PVDF gel electrolyte film and  $BaTiO_3$  separator film using the Nyquist curves, the equivalent series resistance (ESR) was 306  $\Omega$  and 125  $\Omega$ , respectively. The paper supercapacitor based on  $BaTiO_3$  gel separator structure represents a new type of flexible supercapacitor with high performance that can be applied to electronic devices.

**Keywords** Flexible · Supercapacitor · Gel electrolyte · Graphite nanoparticles

## Introduction

Supercapacitors with high power levels due to long cycle life, short time of charge/discharge and low cost are very useful in applications such as transport and energy recovery. In many industries with fluctuating loads, supercapacitors have increasingly played the role of the stabilizer for the power supply and voltage [1]. Supercapacitors are suitable for energy harvesting systems that are used to power an integrated circuit [2]. A large application of supercapacitors is needed in the transport such as power emergency actuators

in airliners (doors and evacuation slides) and high specific power in military vehicles (radar, power supplies for laser and airbag, radio communications, etc.) [3, 4]. Supercapacitors are commonly used in hybrid electric vehicles (HEV) as a fuel reduction of brake energy due to a number of favorable properties [5]. These include fast charge, longer lifetime, stable electrical properties and broader temperature range. A flexible supercapacitor is necessary for both portable and wearable electronic during folding and twisting conditions. A supercapacitor is made of two electrodes, an electrolyte and a separator that due to charge storage method divided into pseudocapacitors, electrical double layer capacitors (EDLCs) and hybrid supercapacitors. The mechanism of charge storage in EDLCs is based on the energy storage at the electrode/electrolyte interface and depends on the contact surface between the electrolyte and electrode. The electrodes of EDLCs are made using metal oxides, lithium ion materials and conducting polymers. But currently due to large surface areas, lightweight, electrochemical stability and excellent conductivity of carbon nanotubes (CNTs), activated carbon and graphene are widely used [6, 7]. The mechanism of charge storage in pseudocapacitors is based on the Faradic reactions (oxidation–reduction reactions),

✉ L. Fekri Aval  
leila2mst@yahoo.com

M. Ghoranneviss  
m\_ghoranneviss29@yahoo.com

G. Behzadi Pour  
ghobadbehzadi@yahoo.com

<sup>1</sup> Plasma Physics Research Center, Science and Research Branch, Islamic Azad University, P.O. Box 14665-679, Tehran, Iran

<sup>2</sup> Department of Physics, East Tehran Branch, Islamic Azad University, Tehran, Iran

store energy near the surface and within the bulk of the electrodes [8]. The electrodes of pseudocapacitors are made using transition metal oxides and conducting polymers along with their composites. The lifetime of Faradaic capacitors is shorter than EDLCs. Hybrid supercapacitors combine pseudocapacitors with EDLCs using asymmetric electrodes [9]. In hybrid supercapacitors, one electrode contains a material that conducts a pseudocapacitors mechanism and at the second electrode, charge separation occurs due to EDLCs formation. Supercapacitor based on the electrolyte divided into gel-state electrolytes, solid-state electrolytes, and liquid-state electrolytes. Supercapacitors based on solid-state prevent leakage. There is normally a poor contact between the electrode and the electrolyte. Leakage is also an important problem in liquid-state electrolytes. Therefore, during the development of supercapacitors, the gel-state electrolytes are commonly used [10, 11]. Recently, carbon nanomaterials because of conductivity and other excellent features could replace charge collectors in supercapacitors. The larger specific surface area (SSA) of CNTs ( $430\text{--}1600\text{ m}^2\text{ g}^{-1}$ ) as an electrode in supercapacitor displays the higher specific capacitance. The specific capacitance of CNTs greatly depends on the purity and the morphology of the electrode surface material [12]. The specific capacitance of purified CNTs is in the range of  $20\text{--}80\text{ F g}^{-1}$  and can be increased by the oxidative process [13]. The results of paper supercapacitor analysis based on multi-wall carbon nanotubes (MWCNTs) electrodes and electrolyte by  $\text{H}_3\text{PO}_4$  and PVA has been reported by Shieh et al. [14]. They showed the specific capacitance was  $47\text{ F g}^{-1}$ . In Ref. [15], a flexible paper based on single-wall carbon nanotubes (SWCNTs) supercapacitor with  $\text{H}_3\text{PO}_4/\text{PVA}$  electrolyte has been investigated. In their study, the specific capacitance was reported as  $115\text{ F g}^{-1}$ . In another study, the paper supercapacitor with SWCNTs/graphene composites has been studied by Li et al. [16]. They reported the specific capacitance for SWCNTs as  $36\text{ F g}^{-1}$  and that for composites film as  $100\text{ F g}^{-1}$ . Ping et al. [17] compared the 2D graphene paper and the 3D graphene foam electrodes and showed the specific capacitances were  $82.9$  and  $128\text{ F g}^{-1}$ , respectively. A high-performance supercapacitor based on the fine sandpaper-based electrodes and a microporous separator coated with a  $\text{H}_3\text{PO}_4/\text{PVA}$  gel electrolyte and graphene/MWCNTs electrode has been reported by Yu et al. [18]. They showed that at the voltage scan rate  $20\text{ mV s}^{-1}$ , the specific capacitance of the sandpaper-based supercapacitor was  $55\text{ F g}^{-1}$ . Activated carbon is widely used for electrodes in supercapacitors due to its SSA ( $1000\text{--}3500\text{ m}^2\text{ g}^{-1}$ ) and low cost. In Ref. [19], the specific capacitance of supercapacitor based on activated carbon electrode for aqueous electrolyte and organic electrolyte has been reported. They reported the specific capacitance based on an activated carbon electrode for aqueous electrolyte and organic electrolyte as  $< 200\text{ F g}^{-1}$  and  $<$

$100\text{ F g}^{-1}$ , respectively. Saha et al. [20] reported the specific capacitance of supercapacitor based on mesoporous carbon as  $102\text{ F g}^{-1}$ . There are different methods to synthesize the mesoporous carbons such as high-degree activation and carbonization of precursors and aerogels [21]. Paper with low cost and environmentally friendly is a suitable substrate for the advance of a flexible supercapacitor [22]. In this study, the fabrication of paper supercapacitor based on GNPs electrodes and gel electrolyte has been investigated. The PVDF and  $\text{PVA}/\text{H}_3\text{PO}_4$  were used as a gel electrolyte. The PVA/water and  $\text{BaTiO}_3$  were used as a gel separator film. The different layer of the paper supercapacitors using TEM and SEM analyses has been characterized as well. The electrical capacitance of the paper supercapacitors based on different gel electrolytes using CV and galvanostatic methods has been reported. Also, the Nyquist curve and Bode curve of the paper supercapacitors have been measured using electrochemical impedance spectroscopy.

## Materials and methods

In this study, a piece of white regular paper ( $3\times 6\text{ cm}$ ) as a substrate was used. At first, on the substrate using the push coating, a film of PVDF gel electrolyte has been coated. The PVDF gel electrolyte was prepared by mixing PVDF ( $10\text{ g}$ ) with *N*-methyl-2-pyrrolidone (NMP:  $10\text{ mL}$ ). This solution was dispersed by magnetic stirring for  $30\text{ min}$ . The gel electrolyte was pushed on the paper using a roller. The PVA gel electrolyte was prepared by mixing PVA ( $1\text{ g}$ ) with deionized water ( $10\text{ mL}$ ). This solution was mixed by magnetic stirring at  $90\text{ }^\circ\text{C}$  to thoroughly dissolve the PVA in the water for  $2\text{ h}$ . Then,  $\text{H}_3\text{PO}_4$  ( $4.7\text{ g}$ ) was added into the stirred PVA solution. Then, the paper with gel electrolyte was dried in an oven at  $60\text{ }^\circ\text{C}$  for  $30\text{ min}$ . On the gel electrolyte film, using push coating, a layer of GNPs has been coated. In the Fig. 1a, the TEM image of the GNPs has been displayed. The average size of GNPs diameter analyzed by Simagis Live [23] was  $39\text{ nm}$ . The SEM image of the GNPs has been presented in Fig. 1b. The CV, galvanostatic and EIS curves of the paper supercapacitors based on different gel electrolytes have been measured using ZIVE SP1 potentiostat/galvanostat.

## Results and discussion

In this letter, three-type paper supercapacitors with the different structures have been fabricated. The schematic of the paper supercapacitor with the structure of PVDF gel electrolyte and GNPs electrodes is illustrated in Fig. 2a. Figure 2b shows the paper with gel electrolyte film in the oven. Schematic of the push coating method and the images of

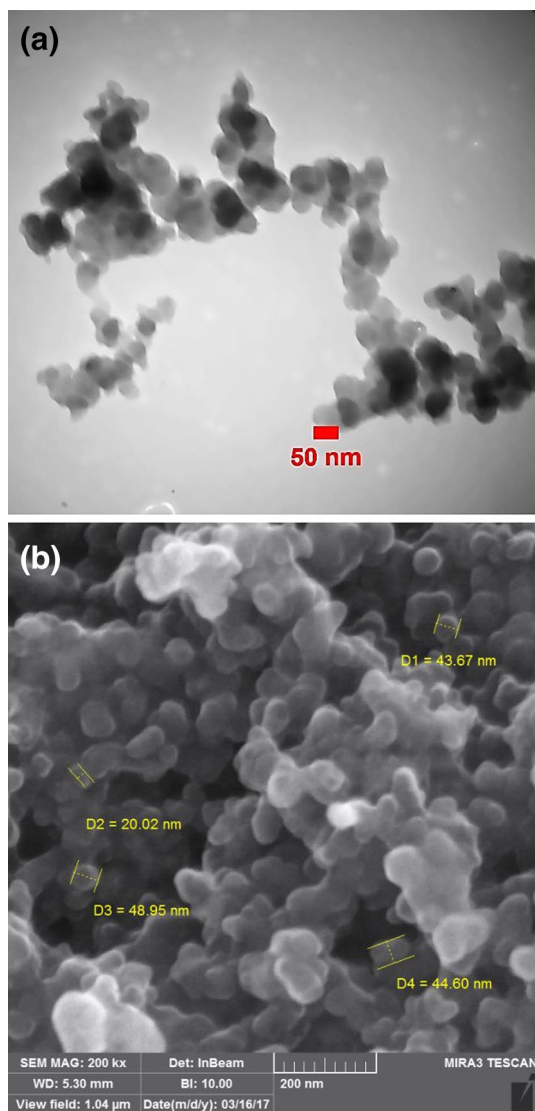


**Fig. 1** a TEM image of GNPs, b SEM image of GNPs

the fabricated paper supercapacitor have been illustrated in Fig. 2c, d. The SEM images of the paper surface before and after gel electrolyte coating are presented in Fig. 3a, b. As it can be seen in Fig. 3c, the morphology of the paper surface indicated that the pores of the surface were filled with gel electrolyte. Using the push coating method, a layer of GNPs has been coated on the gel electrolyte film. The SEM images of GNPs electrode surface morphology have been displayed in Fig. 4 as well. The CV curves of paper supercapacitor based on PVDF gel electrolyte and GNPs electrodes are presented in Fig. 5a. The voltage scan rates were  $20 \text{ mV s}^{-1}$  and  $150 \text{ mV s}^{-1}$  also the potential range was  $-1 \text{ V}$  to  $+1 \text{ V}$ . The CV curve of paper supercapacitor at the voltage scan rate  $150 \text{ mV s}^{-1}$  showed a nearly rectangular shape. As it can be seen in Fig. 5a, the current changes for the voltage scan rate  $150 \text{ mV s}^{-1}$  was from  $-0.8 \text{ A}$  to  $1.34 \text{ A}$  and for

the voltage scan rate  $20 \text{ mV s}^{-1}$  was from  $-0.3 \text{ A}$  to  $0.56 \text{ A}$ . The specific capacitance of the paper supercapacitors using CV curves can be obtained from the following formula [24]:

$$C_m = \frac{\int_{V_1}^{V_2} I dV}{mS(V_2 - V_1)}, \quad (1)$$

where  $m$  is the mass of the electrode materials,  $I$  is the current in the CV curve and  $S$  is the voltage scan rate. From Eq. (1) the specific capacitance of paper supercapacitor for voltage scan rate  $150 \text{ mV s}^{-1}$  was  $42 \text{ F g}^{-1}$  and for voltage scan rate  $20 \text{ mV s}^{-1}$  was  $176 \text{ F g}^{-1}$ . As the results demonstrated, the specific capacitance of the paper supercapacitor was increased with a decreasing voltage scan rates. This behavior is related to the porous structure of the electrode nano-materials in paper supercapacitor [25]. The galvanostatic charge–discharge curves (five cycles) for paper supercapacitor based on PVDF gel electrolyte and GNPs electrodes, with current density  $0.06 \text{ mA cm}^{-2}$  are shown in Fig. 5b. The specific capacitance of the paper supercapacitor using charge–discharge method can be obtained by the below formula [26]:

$$C_m = \frac{I}{m \left( \frac{dV}{dt} \right)}, \quad (2)$$

where  $I$  is the constant current,  $dV/dt$  is the absolute value of the slope of the discharging curve and  $m$  is the mass of the active materials. Using the charge–discharge curve and Eq. 2, the specific capacitance of the paper supercapacitor based on PVDF gel electrolyte was  $152 \text{ F g}^{-1}$ . This value is inside the range of the specific capacitances of CV curves ( $42\text{--}176 \text{ F g}^{-1}$ ).

The schematic of the paper supercapacitor with the structure PVA gel separator film and GNPs electrodes is shown in Fig. 6a. In the second structure of the paper supercapacitor, a layer of the PVA gel separator has been coated on the PVDF gel electrolyte film. The solution of PVA/water without  $\text{H}_3\text{PO}_4$  produces a gel dielectric that creates a separator film in paper supercapacitors. Then, a layer of PVA gel electrolyte has been coated on the gel separator film. Comparison of SEM images of PVDF film surface, PVA gel separator film and PVA gel electrolyte film is shown in Fig. 7. On the gel electrolyte film, using push coating, a layer of GNPs has been coated. The CV curves of paper supercapacitor based on PVA gel separator film and GNPs electrodes are presented in Fig. 8a. As it can be seen in Fig. 8a, the current changes for the voltage scan rate  $150 \text{ mV s}^{-1}$  was from  $-1.8 \text{ A}$  to  $2 \text{ A}$  and for the voltage scan rate  $20 \text{ mV s}^{-1}$  was from  $-0.66 \text{ A}$  to  $0.56 \text{ A}$ . From Eq. (1), the specific capacitance of paper supercapacitor based on PVA gel separator film for voltage scan

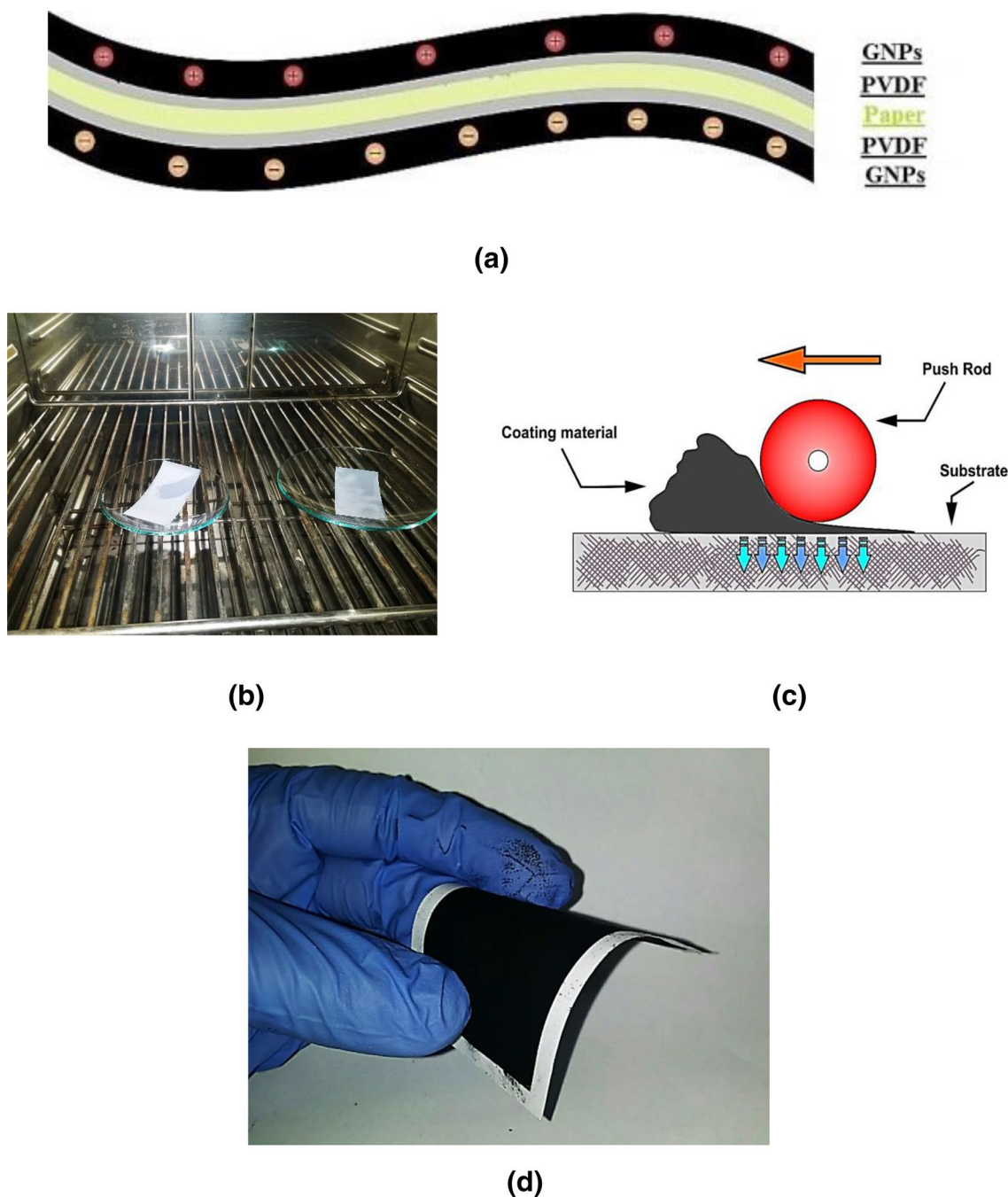
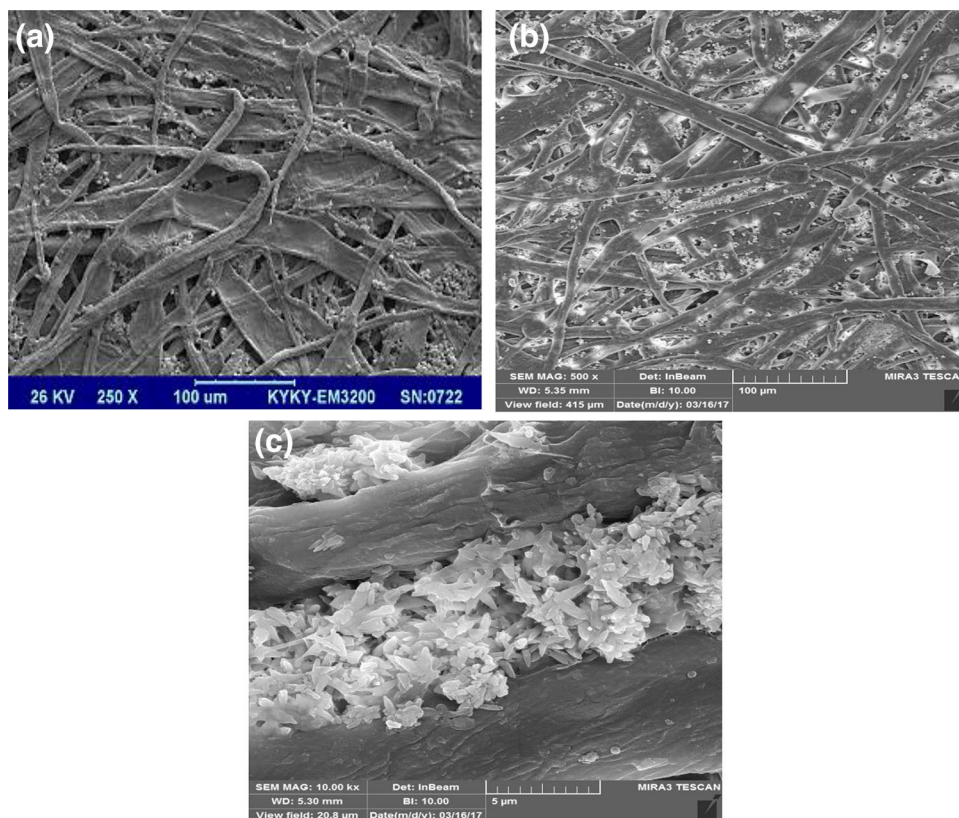


**Fig. 2** **a** Schematic of the paper supercapacitor with the structure of PVDF/NMP gel electrolyte and GNPs electrodes, **b** paper with gel electrolyte film in the oven, **c** schematic of the push coating method, **d** image of the fabricated paper supercapacitor

rate  $150 \text{ mV s}^{-1}$  was  $102 \text{ F g}^{-1}$  and for voltage scan rate  $20 \text{ mV s}^{-1}$  was  $263 \text{ F g}^{-1}$ . The schematic of the paper supercapacitor with the structure of  $\text{BaTiO}_3$  gel separator film and GNPs electrodes is shown in Fig. 6b. In the third structure of the paper supercapacitor, a layer of the  $\text{BaTiO}_3$  gel separator has been coated on the PVA gel separator film. The SEM images of  $\text{BaTiO}_3$  gel separator film surface are shown in Fig. 7d. For better comparison, the

CV curves of the paper supercapacitor based on  $\text{BaTiO}_3$  gel separator film and GNPs electrodes also are presented in Fig. 8a. The current change for the voltage scan rate  $150 \text{ mV s}^{-1}$  was from  $-1.64 \text{ A}$  to  $2.22 \text{ A}$  and for the voltage scan rate  $20 \text{ mV s}^{-1}$  was from  $-0.4 \text{ A}$  to  $0.79 \text{ A}$ . From Eq. (1), the specific capacitance of paper supercapacitor based on  $\text{BaTiO}_3$  gel separator film for voltage scan rate  $150 \text{ mV s}^{-1}$  was  $117 \text{ F g}^{-1}$  and for voltage scan rate  $20 \text{ mV}$

**Fig. 3** SEM images of paper surface **a** before and **b** after gel electrolyte coating, **c** morphology of paper surface with gel electrolyte in 5  $\mu\text{m}$  scale



$\text{s}^{-1}$  was  $312 \text{ F g}^{-1}$ . Comparison of paper supercapacitors shows that the specific capacitance of the  $\text{BaTiO}_3$ -based supercapacitor is higher than the PVA-based supercapacitor. The galvanostatic charge–discharge curves (five cycles) for paper supercapacitor based on PVA gel separator film and GNPs electrodes are shown in Fig. 8b. Using the charge–discharge curve and Eq. 2, the specific capacitance of the paper supercapacitor based on PVA gel separator film was  $300 \text{ F g}^{-1}$ . For better comparison, the galvanostatic charge–discharge curves (five cycles) for paper supercapacitor based on  $\text{BaTiO}_3$  gel separator film and GNPs electrodes also are illustrated in Fig. 8b. Using the charge–discharge curve and Eq. 2, the specific capacitance of the paper supercapacitor based on  $\text{BaTiO}_3$  gel separator film was  $320 \text{ F g}^{-1}$ . In energy storage devices, a low internal resistance ( $iR_{\text{drop}}$ ) is important because less energy wasted to generate heat during the charge/discharge process [14]. The charge/discharge curves of the paper supercapacitors at applied current 1 mA are shown in Figs. 5b and 8b. The charge/discharge curves show that due to internal resistance, almost no  $iR_{\text{drop}}$  was observed. This behavior is related to a very low ESR of GNPs film-based supercapacitor. Xie et al. [27] reported the compact-designed supercapacitors using free-standing SWCNT films. They showed that for SWCNT film-based supercapacitor at  $0.75 \text{ A g}^{-1}$  and potential window (0–3 V), no obvious  $iR_{\text{drop}}$  was observed in the charge/discharge

curve. The equivalent circuit of the paper supercapacitor is shown in Fig. 9.

The energy density and the power density can be obtained from [28]:

$$E (\text{Wh kg}^{-1}) = \frac{1}{2} \frac{1000}{3600} C_S V^2, \quad (3)$$

$$P (\text{Wh kg}^{-1}) = \frac{E \times 3600}{t}, \quad (4)$$

where  $C_S$  is the specific capacitance,  $V$  is the potential window in the discharge process and  $t$  is the discharge time. The energy density and power density of the PVDF-based supercapacitor were  $36 \text{ Wh kg}^{-1}$  and  $7 \text{ kW kg}^{-1}$ , respectively. For PVA-based supercapacitor and  $\text{BaTiO}_3$ -based supercapacitor, the energy densities were  $62 \text{ Wh kg}^{-1}$  and  $65 \text{ Wh kg}^{-1}$  and power densities were  $10 \text{ kW kg}^{-1}$  and  $11 \text{ kW kg}^{-1}$ , respectively. The equivalent circuit of the supercapacitor considered as a capacitor ( $C$ ) in parallel with the resistance ( $R_x$ ). The theoretical capacitance can be obtained by [29]:

$$C = \epsilon_g \left( \frac{\epsilon_0 A}{t_g} \right), \quad (5)$$

where  $\epsilon_g$  is the relative permittivity of the gel electrolyte,  $\epsilon_0$  is the permittivity of the free space,  $t_g$  is the thickness of the

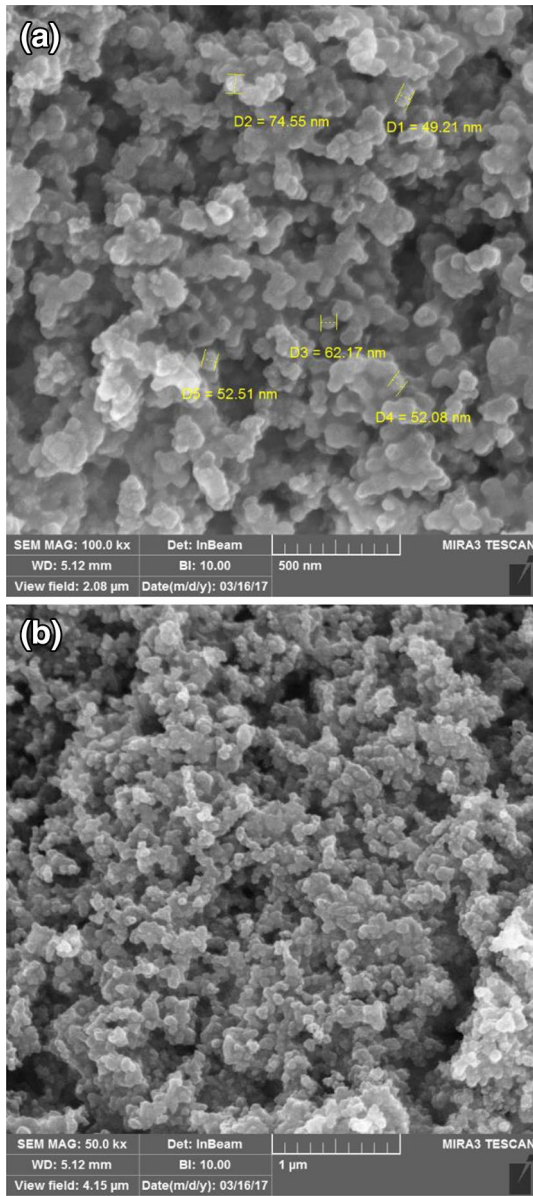


Fig. 4 SEM images of GNPs film surface in scales a 500 nm, b 1 μm

gel electrolyte and  $A$  is the area of the GNPs electrode. The relative permittivity due to the electrical conductivity of the gel electrolyte film is complex. The relative complex permittivity for a lossy medium can be obtained from the real part and the imaginary part. The relative complex permittivity is given by [29]:

$$\epsilon_{ox} = \epsilon'_{ox} + j\epsilon''_{ox}, \tag{6}$$

where the first part of the Eq. (6) is the real part and the second part of the Eq. (6) is the imaginary part which results in the reactance capacitance of the gel electrolyte. The reactance capacitance is caused by a self-discharge in the supercapacitors. The equivalent series resistance (ESR) is series

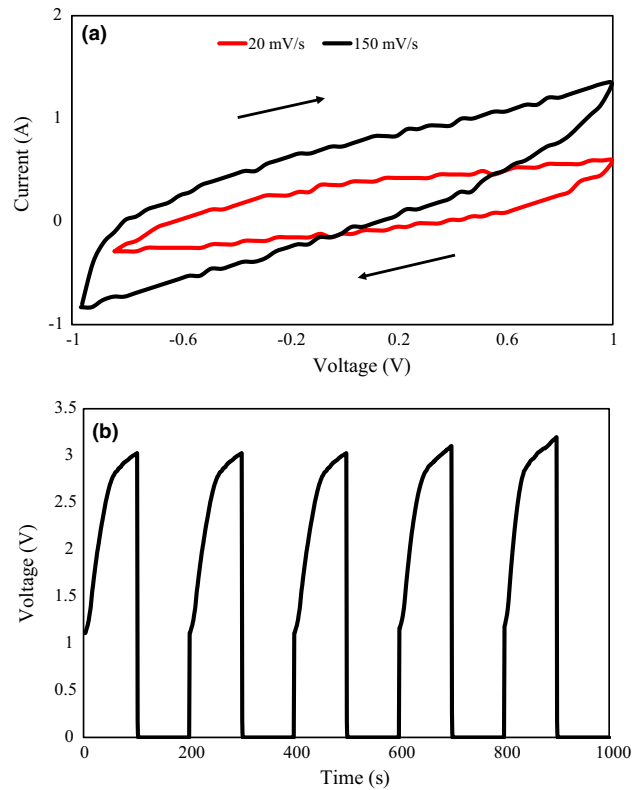


Fig. 5 a Cyclic voltammetry (CV) at 20 mV s<sup>-1</sup> and 150 mV s<sup>-1</sup>, b galvanostatic charge–discharge results from paper supercapacitor with PVDF gel electrolyte and GNPs electrodes

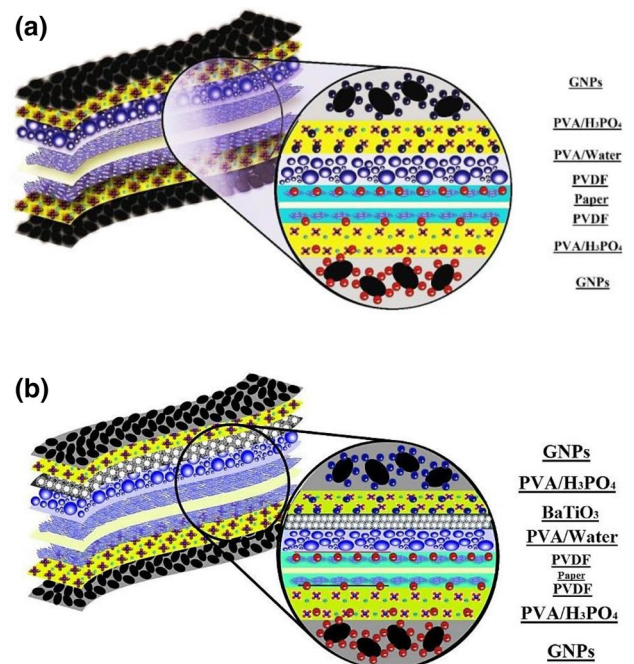
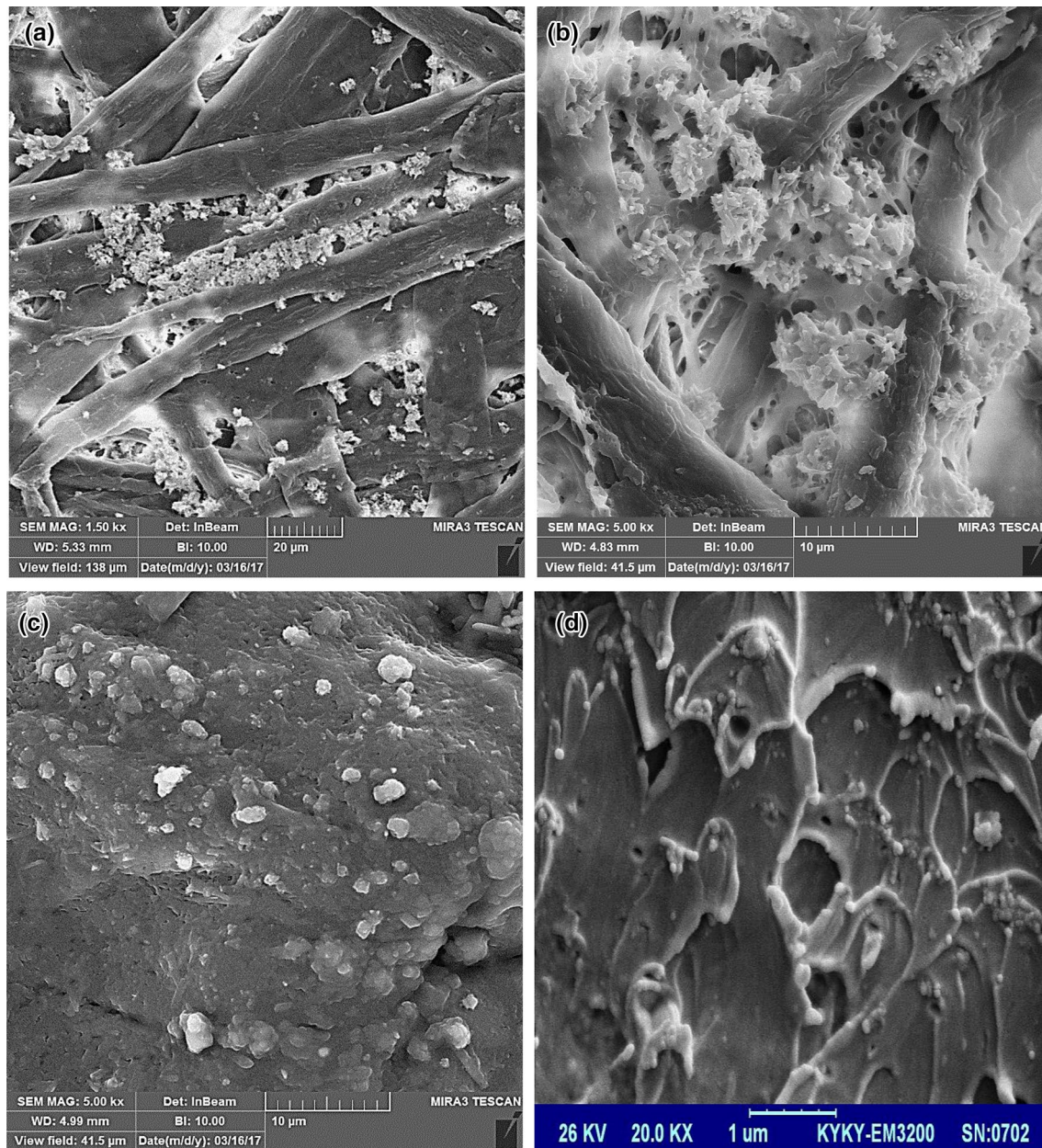


Fig. 6 Schematic of the paper supercapacitor with the structure of a PVA gel separator film and GNPs electrodes, b BaTiO<sub>3</sub> gel separator film and GNPs electrodes



**Fig. 7** SEM images of **a** PVDF gel electrolyte film, **b** PVA gel separator film, **c** PVA gel electrolyte film, **d** BaTiO<sub>3</sub> gel separator film

with the capacitor and is due to resistance of the electrode surfaces. For the paper supercapacitors, the electrochemical impedance spectroscopy (EIS) was measured to calculate the internal resistance. The EIS was done at a dc bias of 10 mV with the frequency range of 100 kHz~10 mHz. For the paper supercapacitor based on PVDF gel electrolyte and GNPs electrodes, the Nyquist curve is plotted in Fig. 10a. The Nyquist curve allows us to determine the ESR resistance and  $R_x$  of the supercapacitor. In the 100 kHz frequency, the real part of the impedance was denoted as ESR. The resistance  $R_x$  can be obtained from the semicircular part. For the paper supercapacitor based on PVDF gel electrolyte, the

ESR resistance and  $R_x$  were 306  $\Omega$  And 44  $\Omega$ , respectively. As it can be seen in Fig. 10a, the semicircular part of the Nyquist curve has been flattened. It is due to the fact that the electrode surface is uneven. The curve slope is related to the Warburg resistance that is due to the frequency dependency of the diffusion from the electrolyte to the electrode [30]. The impedance variations as the function of frequency are shown in Fig. 10b. The Bode curve shows that by increasing the frequency from 10 mHz to 100 kHz, the impedance was decreased from 2.6 k $\Omega$  to 307  $\Omega$ . For the paper supercapacitor based on PVA gel separator film and GNPs electrodes, the Nyquist curve is plotted in Fig. 10c. From Fig. 10c, the

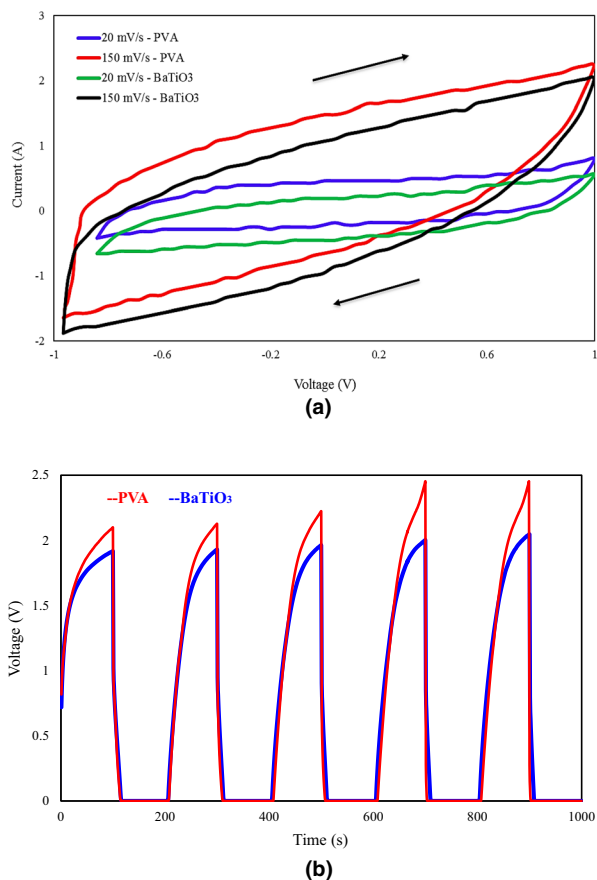


**Fig. 8** a Cyclic voltammetry (CV) at 20 mV s<sup>-1</sup> and 150 mV s<sup>-1</sup>, b galvanostatic charge–discharge results from paper supercapacitor with PVA and BaTiO<sub>3</sub> gel separator film

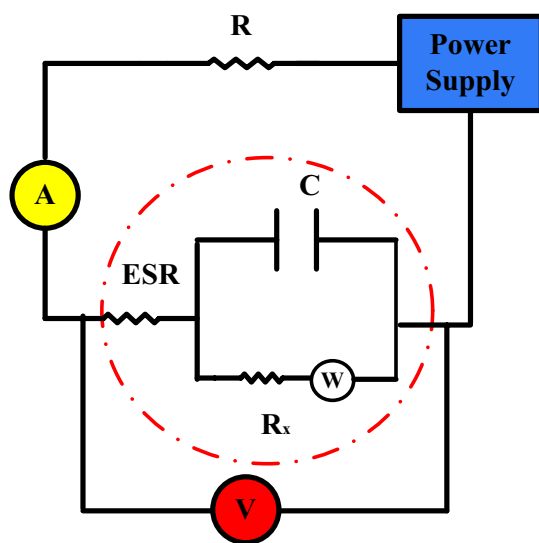


**Fig. 9** Schematic of equivalent circuit of the paper supercapacitor

ESR resistance and  $R_x$  were 72  $\Omega$  and 26  $\Omega$ , respectively. At the high frequency, the semicircular part of the Nyquist curve is demonstrated in Fig. 10c. The Bode curve of paper supercapacitor based on the PVA gel separator is shown in Fig. 10d. By increasing the frequency from 10 mHz to 100 kHz, the impedance is decreased from 1.3 k $\Omega$  to 72  $\Omega$ . For the paper supercapacitor based on BaTiO<sub>3</sub> gel separator film and GNPs electrodes, the Nyquist curve is plotted in Fig. 10e. The ESR resistance and  $R_x$  were 125  $\Omega$  and 525  $\Omega$ , respectively. The Bode curve of paper supercapacitor based on the BaTiO<sub>3</sub> gel separator is shown in Fig. 10f. By increasing the frequency from 10 mHz to 100 kHz, the impedance was decreased from 2.45 k $\Omega$  to 170  $\Omega$ . The comparison of different supercapacitor based on the PVDF and PVA gel electrolyte is illustrated in Table 1. As indicated in Table 1, the specific capacitance of the paper supercapacitor based on the GNPs electrode and PVA gel electrolyte is much more than paper supercapacitor based on the MWCNTs and SWCNTs electrodes [10, 14–16, 31]. In Ref. [32], a polyester paper supercapacitor based on the MWCNTs electrode and PVA electrolyte has been reported. At it is shown, the specific capacitance of the paper supercapacitor was 276 F g<sup>-1</sup> in scan rate 5 mV s<sup>-1</sup>. Hu et al. [33] indicated the specific capacitance of paper supercapacitor based on the PVDF gel electrolyte was 33 F g<sup>-1</sup>. The comparison of PET substrate supercapacitors is shown in Table 1 [34–36]. The specific capacitance of PET substrate supercapacitor based on the SWCNTs electrode and PVA gel electrolyte was 36 F g<sup>-1</sup>. Wang et al. [37] reported the specific capacitance of supercapacitor based on piezoelectric PVDF film and PVA gel electrolyte with carbon fiber electrode as 357 F m<sup>-2</sup>. For the paper supercapacitor based on the KCu<sub>7</sub>S<sub>4</sub>/graphene electrode and PVA electrolyte, the specific capacitance was 483 F g<sup>-1</sup> [38].

## Conclusion

In this paper, three-type paper supercapacitors with the different structures have been fabricated. The morphology of electrolyte surfaces and GNPs has been characterized using SEM and TEM. The CV curves of paper supercapacitors based on different gel electrolyte and GNPs electrodes also have been investigated. The voltage scan rates were 20 mV s<sup>-1</sup> and 150 mV s<sup>-1</sup> and the potential range was -1–1 V. The CV curve of the paper supercapacitor at the voltage scan rate 150 mV s<sup>-1</sup> showed nearly rectangular shape. The specific capacitance of paper supercapacitor based on PVDF gel electrolyte for voltage scan rate 150 mV s<sup>-1</sup> was 42 F g<sup>-1</sup> and for voltage scan rate 20 mV s<sup>-1</sup> was 176 F g<sup>-1</sup>. In the second structure of the paper supercapacitor, a layer of the PVA gel separator has been coated on the PVDF gel electrolyte film. The specific capacitance of paper supercapacitor based



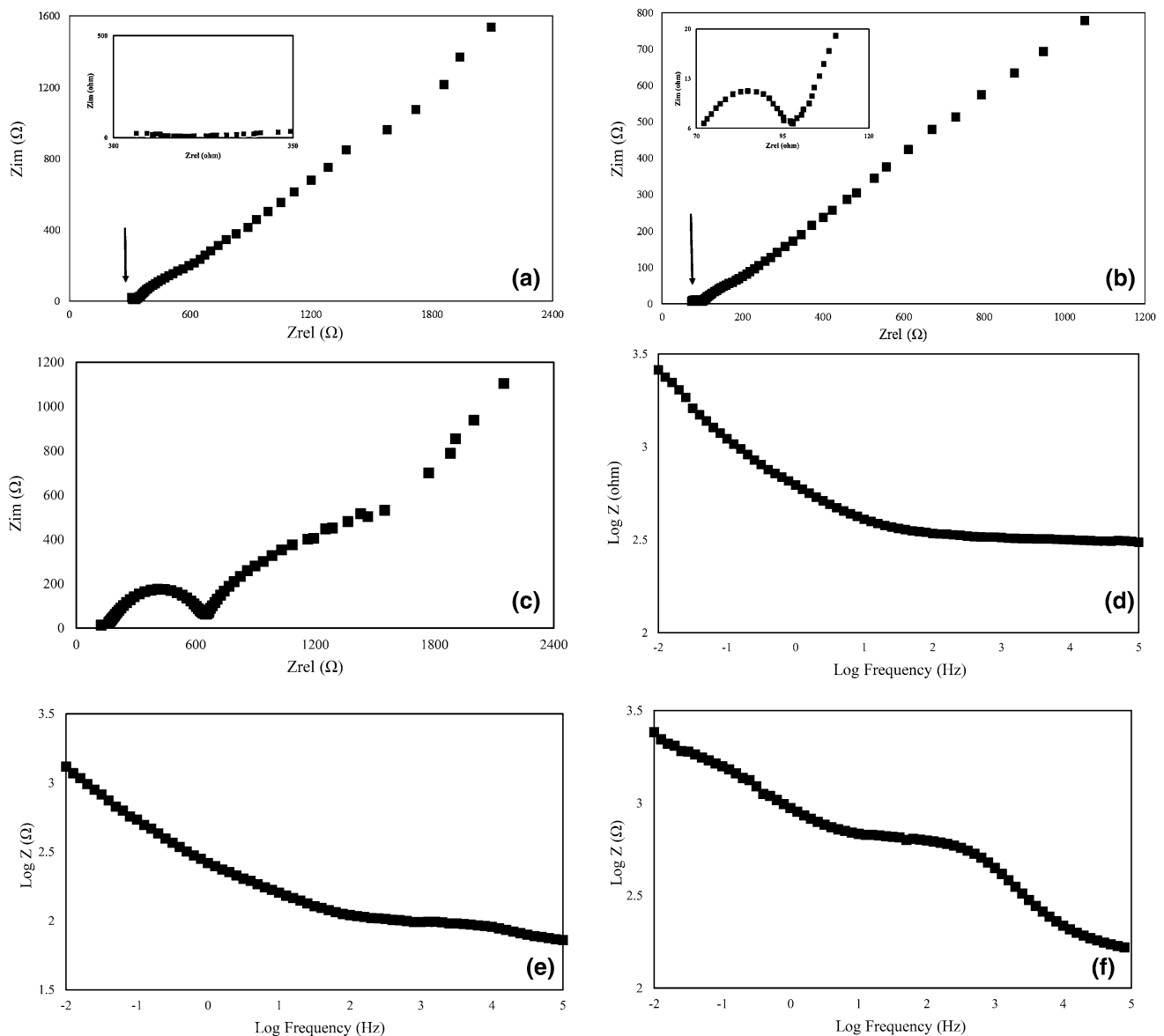


**Fig. 10** The Nyquist curves of the paper supercapacitors based on **a** PVDF gel electrolyte, **b** PVA gel separator, **c** BaTiO<sub>3</sub> gel separator, and the Bode curves of the paper supercapacitors based on **d** PVDF gel electrolyte, **e** PVA gel separator, **f** BaTiO<sub>3</sub> gel separator

on PVA gel separator film for voltage scan rate 150 mV s<sup>-1</sup> and 20 mV s<sup>-1</sup> were 102 F g<sup>-1</sup> and 263 F g<sup>-1</sup>, respectively. In the third structure of the paper supercapacitor, a layer of the BaTiO<sub>3</sub> gel separator has been coated on the PVA gel separator film. The specific capacitance of paper supercapacitor based on BaTiO<sub>3</sub> gel separator film for voltage scan rate 150 mV s<sup>-1</sup> was 117 F g<sup>-1</sup> and for voltage scan rate 20 mV s<sup>-1</sup> was 312 F g<sup>-1</sup>. Using the galvanostatic method, the specific capacitance of the paper supercapacitor based on BaTiO<sub>3</sub> gel separator film was 320 F g<sup>-1</sup>. The EIS analysis was done at a dc bias of 10 mV with the frequency range of

100 kHz–~ 10 mHz. The Nyquist curve allows us to determine the ESR resistance and  $R_x$  of the supercapacitor. For the paper supercapacitor based on PVDF gel electrolyte, the ESR resistance and  $R_x$  were 306 Ω And 44 Ω, respectively. The ESR resistance and  $R_x$  of the paper supercapacitor based on BaTiO<sub>3</sub> gel separator film were 125 Ω and 525 Ω, respectively. From the Bode curve of the paper supercapacitor based on the BaTiO<sub>3</sub> gel separator by increasing the frequency from 10 mHz to 100 kHz, the impedance was decreased from 2.45 kΩ to 170 Ω. Our results demonstrated that the flexible solid state paper supercapacitor based on BaTiO<sub>3</sub> gel separator film showed the excellent performance that could be applied in energy storage devices.

**Table 1** Comparison of different supercapacitor based on the PVDF and PVA gel electrolytes

Substrate	Electrodes	Electrolyte	Specific capacitance	Scan rate (mv s <sup>-1</sup> )	References
Paper	GNPs	PVDF	176 F g <sup>-1</sup>	20	This work
Paper	GNPs	PVDF + PVA	263 F g <sup>-1</sup>	20	This work
Paper	GNPs	PVDF + PVA/BaTiO <sub>3</sub>	312 F g <sup>-1</sup>	20	This work
Porous polydimethylsiloxane	MWCNTs/graphene	PVA	96 F g <sup>-1</sup>	20	[10]
Sandpaper	MWCNTs/graphene	PVA	55 F g <sup>-1</sup>	20	[10]
Paper	MWCNTs	PVA	47 F g <sup>-1</sup>	50	[14]
Paper	SWCNTs	PVA	115.8 F g <sup>-1</sup>	< 10	[15]
Paper	SWCNTs	PVDF/KOH	36 F g <sup>-1</sup>	10	[16]
Paper	SWCNTs/graphene	PVDF/KOH	100 F g <sup>-1</sup>	10	[16]
Paper	MWCNTs	PVA	219 F g <sup>-1</sup>	20	[27]
Paper	Carbon blacks	PVA	92 F g <sup>-1</sup>	20	[27]
Polyester paper	MWCNTs	PVA	276 F g <sup>-1</sup>	5	[28]
Paper	SWCNTs	PVDF	33 F g <sup>-1</sup>	–	[29]
PET	Graphene	PVA	2.6 mF cm <sup>-2</sup>	100	[30]
PET	Graphene	PVA	12.4 μF cm <sup>-2</sup>	10	[31]
PET	SWCNTs	PVA	36 F g <sup>-1</sup>	10	[32]
Piezoelectric PVDF film	Carbon fibers	PVA	357.6 F m <sup>-2</sup>	10	[33]
Paper	KCu <sub>7</sub> S <sub>4</sub> /graphene	PVA	483 F g <sup>-1</sup>	–	[34]

**Acknowledgements** This research work was financially supported by the Iran National Science Foundation (INSF) and Grant number (INSF: 96007938).

**Open Access** This article is distributed under the terms of the Creative Commons Attribution 4.0 International License (<http://creativecommons.org/licenses/by/4.0/>), which permits unrestricted use, distribution, and reproduction in any medium, provided you give appropriate credit to the original author(s) and the source, provide a link to the Creative Commons license, and indicate if changes were made.

## References

- Khan, J., Nasir, U.: Voltage stabilization of hybrid micro-grid using super capacitors. *J. Power Energy Eng.* **3**, 1–9 (2015)
- Lin, Y.L., Kyung, C.M., Yasuura, H., Liu, Y.: *Smart Sensors and Systems*. Springer International Publishing, Switzerland (2015)
- Rafal, K., Morin, B., Roboam, X., Bru, E., Turpin, C., Piquet, H.: Hybridization of an aircraft emergency electrical network: experimentation and benefits validation. In: *Vehicle Power and Propulsion Conference (VPPC)*. IEEE (2010)
- Kady, M.F., Ihns, M., Li, M., Hwang, J.Y., Mousavi, M.F., Chaney, L., Lech, A.T., Kaner, R.B.: Engineering three-dimensional hybrid supercapacitors and microsupercapacitors for high-performance integrated energy storage. *Proc. Natl. Acad. Sci.* **112**, 4233–4238 (2015)
- Burke, A.F.: Batteries and ultracapacitors for electric, hybrid, and fuel cell vehicles. *Proc. IEEE* **95**, 806–820 (2007)
- Lobato, B., Suarez, L., Guardia, L., Centeno, T.A.: Capacitance and surface of carbons in supercapacitors. *Carbon* **122**, 434–445 (2017)
- Afzal, A., Abuilawi, F.A., Habib, A., Awais, M., Waje, S.B., Atieh, M.A.: Polypyrrole/carbon nanotube supercapacitors: technological advances and challenges. *J. Power Sources* **352**, 174–186 (2017)
- Soin, N., Roy, S.S., Mitra, S.K., Thundat, T., McLaughlin, J.A.: Nanocrystalline ruthenium oxide dispersed few layered graphene (FLG) nanoflakes as supercapacitor electrodes. *J. Mater. Chem.* **22**, 14944–14950 (2012)
- Wang, Y., Song, Y., Xia, Y.: *Electrochemical capacitors: mechanism, materials, systems, characterization and applications*. *Chem. Soc. Rev.* **45**, 5925–5950 (2016)
- Shieh, J.Y., Tsai, S.Y., Li, B.Y., Yu, H.H.: High-performance flexible supercapacitor based on porous array electrodes. *Mater. Chem. Phys.* **195**, 114–122 (2017)
- Obeidat, A.M., Gharaibeh, M.A., Obaidat, M.: Solid-state supercapacitors with ionic liquid gel polymer electrolyte and polypyrrole electrodes for electrical energy storage. *J. Energy Storage* **13**, 123–128 (2017)
- Pandolfo, A.G., Hollenkamp, A.F.: Carbon properties and their role in supercapacitors. *J. Power Sources* **157**, 11–27 (2006)
- Talapatra, S., Kar, S., Pal, S.K., Vajtai, R., Ci, L., Victor, P., Shaijumon, M.M., Kaur, S., Nalamasu, O., Ajayan, P.M.: Direct growth of aligned carbon nanotubes on bulk metals. *Nat. Nanotechnol.* **1**, 112–116 (2006)
- Shieh, J.Y., Zhang, S.H., Wu, C.H., Yu, H.H.: A facile method to prepare a high performance solid-state flexible paper-based supercapacitor. *Appl. Surf. Sci.* **313**, 704–710 (2014)
- Hu, S., Rajamani, R., Yu, X.: Flexible solid-state paper based carbon nanotube supercapacitor. *Appl. Phys. Lett.* **100**, 104103–104104 (2012)
- Li, J., Cheng, X., Sun, J., Brand, C., Shashurin, A., Reeves, M., Keidar, M.: Paper-based ultracapacitors with carbon nanotubes-graphene composites. *Appl. Phys. Lett.* **115**, 164301–164305 (2014)

17. Ping, Y., Gong, Y., Fua, Q., Pan, C.: Preparation of three-dimensional graphene foam for high performance supercapacitors. *Prog. Nat. Sci. Mater. Int.* **27**, 177–181 (2017)
18. Shieh, J.Y., Wu, C.H., Tsai, S.Y., Yu, H.H.: Fabrication and characterization of a sandpaper-based flexible energy storage. *Appl. Surf. Sci.* **364**, 21–28 (2016)
19. Zhang, L.L., Zhao, X.S.: Carbon-based materials as supercapacitor electrodes. *Chem. Soc. Rev.* **38**, 2520–2531 (2009)
20. Saha, D., Li, Y., Bi, Z., Chen, J., Keum, J.K., Hensley, D.K., Grappe, H.A., Meyer, H.M., Dai, S., Paranthaman, M.P., Naskar, A.K.: Studies on supercapacitor electrode material from activated lignin-derived mesoporous carbon. *Langmuir* **30**, 900–910 (2014)
21. Gonzalez, A., Goikolea, E., Barrena, J.A., Mysyk, R.: Review on supercapacitors: technologies and materials. *Renew. Sustain. Energy Rev.* **58**, 1189–1206 (2016)
22. Sharifi, F., Ghobadian, S., Cavalcanti, F.R., Hashemi, N.: Paper-based devices for energy applications. *Renew. Sustain. Energy Rev.* **52**, 1453–1472 (2015)
23. Simagis Live Smart Web Pathology: Smart Imaging Technologies Co. (2017). <http://host.simagis.com>
24. Zhang, Y.Z., Wang, Y., Cheng, T., Lai, W.Y., Pang, H., Huang, W.: Flexible supercapacitors based on paper substrates: a new paradigm for low-cost energy storage. *Chem. Soc. Rev.* **44**, 5181–5199 (2015)
25. Yoon, Y., Lee, K., Baik, C., Yoo, H., Min, M., Park, Y., Lee, S.M., Lee, H.: Anti-solvent derived non-stacked reduced graphene oxide for high performance supercapacitors. *Adv. Mater.* **32**, 4437–4444 (2013)
26. Bello, A., Barzegar, F., Momodu, D., Dangbegnon, J., Taghizadeh, F., Fabiane, M., Manyala, N.: Asymmetric supercapacitor based on nanostructured graphene foam/polyvinyl alcohol/formaldehyde and activated carbon electrodes. *J. Power Sources* **273**, 305–311 (2015)
27. Niu, Z., et al.: Compact-designed supercapacitors using free-standing single-walled carbon nanotube films. *Energy Environ. Sci.* **4**, 1440–1446 (2011)
28. Peng, C., Lang, J., Xu, S., Wang, X.: Oxygen-enriched activated carbons from pomelo peel in high energy density supercapacitor. *RSC Adv.* **4**, 54662–54667 (2014)
29. FekriAval, L., Elahi, S.M., Darabi, E., Sebt, S.A.: Comparison of the MOS capacitor hydrogen sensors with different SiO<sub>2</sub> film thicknesses and a Ni-gate film in a 4% hydrogen–nitrogen mixture. *Sens. Actuators B* **216**, 367–373 (2015)
30. Stoller, M.D., Park, S., Zhu, Y., An, J., Ruoff, R.S.: Graphene-based ultracapacitors. *Nano Lett.* **8**, 3498–3502 (2008)
31. Kalam, A., Bae, J.: Low-cost, high-efficiency conductive papers fabricated using multi-walled carbon nanotubes, carbon blacks and polyvinyl alcohol as conducting agents. *ECS J. Solid State Sci. Technol.* **4**, M41–M45 (2015)
32. Karthika, P., Rajalakshmi, N., Dhathathreyan, K.S.: Flexible polyester cellulose paper supercapacitor with a gel electrolyte. *Chem. Phys. Chem.* **14**, 3822–3826 (2013)
33. Hu, L., Wu, H., Cui, Y.: Printed energy storage devices by integration of electrodes and separators into single sheets of paper. *Appl. Phys. Lett.* **96**, 183502–183503 (2010)
34. Chena, Q., Lic, X., Zang, X., Cao, Y., He, Y., Lid, P., Wang, K., Wei, J., Wud, D., Zhu, H.: Effect of different gel electrolytes on graphene based solid-state supercapacitors. *RSC Adv.* **4**, 36253–36256 (2014)
35. Gao, Y., Zhou, Y.S., Xiong, W., Jiang, L.J., Mahjouri-samani, M., Thirugnanam, P., Huang, X., Wang, M.M., Jiang, L., Lu, Y.F.: Transparent, flexible, and solid-state supercapacitors based on graphene electrodes. *APL Mater.* **1**, 012101–012107 (2013)
36. Lust, E., Nurk, G., Janes, A., Arulepp, M., Permann, L., Nigu, P., Moller, P.: Electrochemical properties of nanoporous carbon electrodes. *Condens. Matter Phys.* **5**, 307–328 (2002)
37. Song, R., Jin, H., Li, X., Fei, L., Zhao, Y., Huang, H., Chan, H.L.W., Wang, Y., Chai, Y.: A rectification-free piezo-supercapacitor with a polyvinylidene fluoride separator and functionalized carbon cloth electrodes. *J. Mater. Chem. A* **3**, 14963–14970 (2015)
38. Dai, S., Xu, W., Xi, Y., Wang, M., Gu, X., Guo, D., Hu, C.: Charge storage in KCu<sub>7</sub>S<sub>4</sub> as redox active material for a flexible all-solid-state supercapacitor. *Nano Energy* **19**, 363–372 (2016)

**Publisher's Note** Springer Nature remains neutral with regard to jurisdictional claims in published maps and institutional affiliations.